Tensor network construction for lattice gas models: Hard-core and triangular lattice models

Sergey S. Akimenko*

Department of Chemistry and Chemical Engineering, Omsk State Technical University, Mira Ave. 11, Omsk 644050, Russian Federation

(Received 3 March 2023; accepted 21 April 2023; published 16 May 2023)

The representation of complex lattice models in the form of a tensor network is a promising approach to the analysis of the thermodynamics of such systems. Once the tensor network is built, various methods can be used to calculate the partition function of the corresponding model. However, it is possible to build the initial tensor network in different ways for the same model. In this work, we have proposed two ways of constructing tensor networks and demonstrated that the construction process affects the accuracy of calculations. For demonstration purposes, we have done a brief study of the 4 nearest-neighbor (NN) and 5NN models, where adsorbed particles exclude all sites up to the fourth and fifth nearest neighbors from being occupied by another particle. In addition, we have studied a 4NN model with finite repulsions with a fifth neighbor. In a sense, this model is intermediate between 4NN and 5NN models, so algorithms designed for systems with hard-core interactions may experience difficulties. We have obtained adsorption isotherms, as well as graphs of entropy and heat capacity for all models. The critical values of the chemical potential were determined from the position of the heat capacity peaks. As a result, we were able to improve our previous estimate of the position of the phase transition points for the 4NN and 5NN models. And in the model with finite interactions, we found the presence of two first-order phase transitions and made an estimate of the critical values of the chemical potential for them.

DOI: 10.1103/PhysRevE.107.054116

I. INTRODUCTION

Modern theoretical studies of two-dimensional condensed systems (for example, adsorption layers on the surface of a solid body) are developing toward more complex models, and quite often these are lattice models [1–9]. Usually, the complication is associated with a detailed account of the adsorbed molecule structure, and takes into account more complex types of interactions: Directed, long-range, and multiparticle interactions [2,10–15]. Of great interest is the self-assembly of adsorption monolayers. This is the process of spontaneous association of molecules on the surface into ordered structures due to noncovalent interactions between them [16–18]. Experimental data indicate a rich variety of such structures and a wide range of promising applications [19,20]. However, the self-assembly process and its result depend on many parameters, such as temperature, pressure, geometry and nature of the surface, molecular structure, etc. This significantly complicates the experimental search for systems with the desired behavior.

Traditional methods of statistical physics, such as Monte Carlo, transfer-matrix, and cluster approximations, do not always allow one to achieve the desired result for models of this type. For example, in the Monte Carlo method, there are problems with achieving equilibrium, and it is possible to calculate only indirect characteristics (for example, the number of certain elements of the structure) [4,10,11,21] or it is necessary to apply specialized algorithms [22–25]. In turn, the transfer-matrix method, like cluster methods, faces serious limitations on the size of the system [26,27]. The unit cells of the ordered structures formed in complex models are quite large, and it is necessary to consider the lattice size multiplicity. Due to the fact that in the transfer-matrix method the complexity of calculations grows exponentially with the size of the system, in some cases the task becomes almost impossible [27]. In addition, the structure of phases and, moreover, the size of unit cells are usually unknown.

A promising approach to the analysis of complex lattice models in the field of statistical physics may be the representation of the model in the form of a tensor network. Some algorithms make it possible to exclude the influence of the finite-size effect, which is difficult to achieve using other methods of statistical physics. In recent years, this approach has been actively developed, but in most works quantum and classical magnetic systems are considered [28–34]. In this regard, the features specific to the field of surface science are usually not taken into account: The size and shape of the molecule, specific types of interactions, etc. Previously, we showed that the direct use of the simplest algorithms allows one to achieve fairly good results in the study of models with exclusions up to kth nearest neighbors (kNN models) [35]. A hard core is the simplest way to account for the size of adsorbed particles. Here we demonstrate how the accuracy of the results obtained for models of this type can be improved without increasing the computational complexity.

The study of lattice models using tensor networks can be divided into two main stages. First, the tensor network is built. For lattice models of adsorption systems, this is usually a two-dimensional tensor network. Next, we need to calculate the partition function, but this cannot be done directly.

*akimenkosergey@mail.ru

Therefore, the next stage is necessary: Calculations using one of the existing numerical methods, such as the tensor renormalization group [36], second renormalization group [37], tensor network renormalization [38], high-order tensor renormalization group [39], corner transfer-matrix renormalization [40,41], etc. [42–44]. Each of them has its own advantages and disadvantages. We will use only the TRG approach since the focus of the work will be on the process of building a tensor network and its impact on the accuracy of the obtained results. The basis of the approach is the iterative contraction of the tensor network. At each iteration, the tensor is reduced to a predetermined value χ. This is based on the process of singular value decomposition, where χ is the number of singular values left at each iteration. The larger the χ value, the higher the accuracy of calculations, but the requirements for computing resources also increase. In Ref. [35] at $\chi = 150$ for 4NN and 5NN models on a triangular lattice, due to lack of accuracy, we managed to calculate only the adsorption isotherm. We assume that one of the reasons is an inefficient algorithm for constructing a tensor network. In this work, we will propose two independent improvements, each of which allows us to increase the accuracy of calculations and retain the same computational complexity, since it does not affect the TRG algorithm itself. The first is the process of building a uniform tensor network for a triangular lattice. This lattice has a more complex structure than the square and hexagonal ones, so we will mainly talk about it. At the same time, some elements of the proposed algorithm can be used in the case of other lattices.

II. CONSTRUCTION OF A TENSOR NETWORK

We will use a graphical representation of operations on tensors, so some explanation should be made. Most often, tensors are depicted as circles with a certain number of rays (often referred to as legs) coming out of them. The number of rays emerging from them characterizes the tensor order. That is, a tensor with one ray is a vector; with two, it is a matrix; and so on. If the tensors have a common ray, then they are contracted along the corresponding dimension. A detailed description of the graphical representation of tensors and operations with them can be found in Ref. [45].

For a more detailed visualization of tensor operations, we will use special C tensor of the nth order, which look like this:

$$C_{x_1,x_2,\ldots,x_n} = \begin{cases} 1 & x_1 = x_2 = \ldots = x_n \\ 0 & \text{otherwise} \end{cases}. \tag{1}$$

For $n = 2$, it is the identity matrix, and for $n > 2$, it is a tensor with ones on the main diagonal. In what follows, we will denote such tensors by small black circles and call them COPY-dots (copydots) [46]. Note that they are convenient for visualizing and describing tensor contractions, but their actual presence in the contraction process is not always necessary.

For the same lattice model, there are different ways to represent the partition function as a tensor network. A simple and universal way is to build through the interaction-round-a-face (IRF) model. It is shown schematically in Fig. 1.

We used the IRF model to build a tensor network in Ref. [35]. The tensor describes the interactions of all neighboring nodes at once and does not take into account the detailed structure of interactions between individual nodes. This can lead to nonoptimality of the initial tensor network.

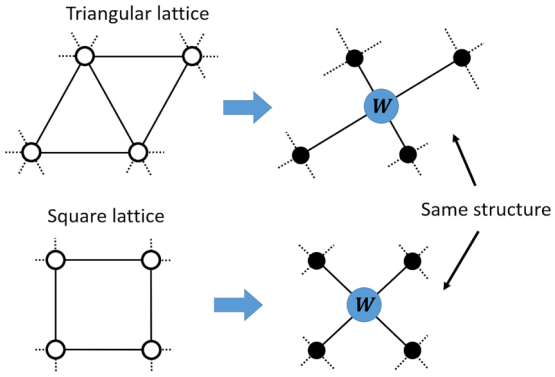

FIG. 1. Building a tensor network using the IRF model.

Another way to build a tensor network is to define a tensor in a dual space [36,47]. In some cases, this approach gives a tensor network with a simple structure. For example, a tensor network consisting of third-order tensors is obtained for classical models on a triangular lattice. At the same time, the process of building a tensor network becomes more complicated for more complex models.

The most visual way is to represent explicitly each element of the lattice structure and connections between nodes in the form of a tensor network. Such a network consists of nth order copydots, where n is equal to the coordination number of the lattice. For example, $n = 6$ for a triangular lattice. Second-order tensors (matrices) $\mathbf{M}$ are located between the copydots. These tensors contain the Boltzmann weights for the linked lattice sites according to the Hamiltonian of a model. Note that for asymmetric models, there will be different matrices $\mathbf{M}$ for different directions. The number of components in all dimensions of the tensor will be the same and we will denote it m. For example, for a classical Ising model with a coupling constant J, the matrix $\mathbf{M}$ will have $m = 2$, and it looks like this:

$$\mathbf{M} = \begin{pmatrix} \exp(\beta J) & \exp(-\beta J) \\ \exp(-\beta J) & \exp(\beta J) \end{pmatrix}, \tag{2}$$

where $\beta = (kT)^{-1}$, k is the Boltzmann constant, and T is the absolute temperature. For simplicity, we will take $\beta = 1$.

One of the standard steps is to get a uniform tensor network. As an example, Fig. 2 graphically shows the process of building a uniform tensor network for square and triangular lattices.

Note that the split of the matrix $\mathbf{M}$ can be done in different ways. For example, you can calculate its square root or perform a division using the singular value decomposition operation. However, a uniform tensor network of a similar structure can be obtained even by direct contraction of tensors. For a triangular lattice, direct contraction will be $T_{abcdef} = \sum_{i,j,k} C_{abcijk}\mathbf{M}_{id}\mathbf{M}_{je}\mathbf{M}_{kf}$.

For a square lattice, a uniform tensor network with fourth-order tensors is obtained. It is suitable for further use of standard algorithms. However, this approach is a bad example for a triangular lattice since the resulting network consists of sixth-order tensors. This leads to a significant increase in

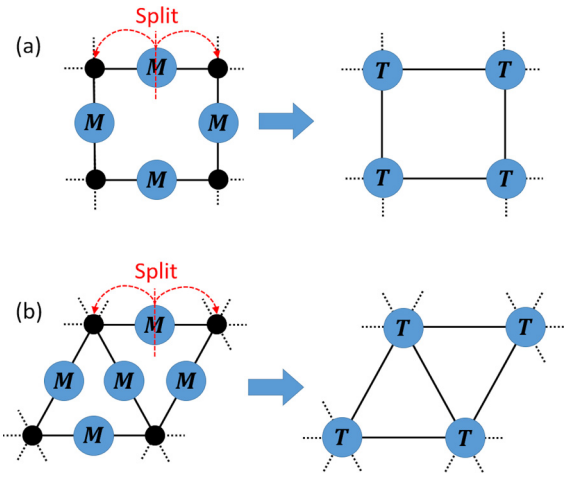

FIG. 2. An example of building a uniform tensor network for (a) square and (b) triangular lattices.

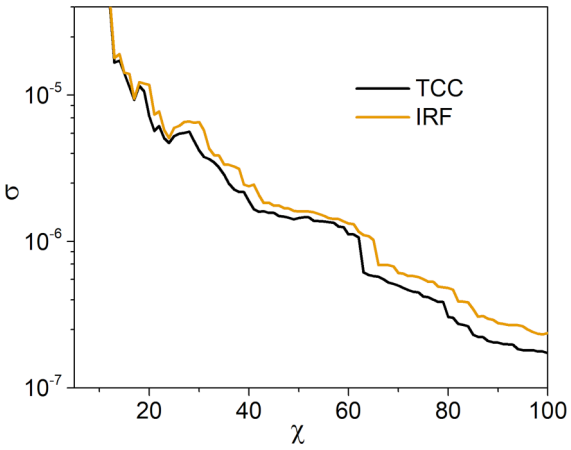

FIG. 4. Dependence of the error value on χ for various ways of constructing a tensor network for the Ising model.

computational complexity in the future. In addition, much more memory is required to store the intermediate and final tensors.

We propose a different approach for constructing a uniform tensor network for a triangular lattice: Tensor contraction with copydots (TCC). Figure 3 shows the visualization of the proposed algorithm.

Note that the construction of a tensor network is performed only through the contraction operations. The result is a uniform tensor network consisting of tensors of the fourth order. And the number of elements of all dimensions remains equal to m. In Ref. [35], we also obtained a fourth-order tensor, but two of its dimensions had the number of components equal to m^2. This can negatively affect the result. It is also important to note that in neither case are there any restrictions on the complexity of the considered models. They can be applied both to hard-core lattice gas models and to ordinary models with finite interactions.

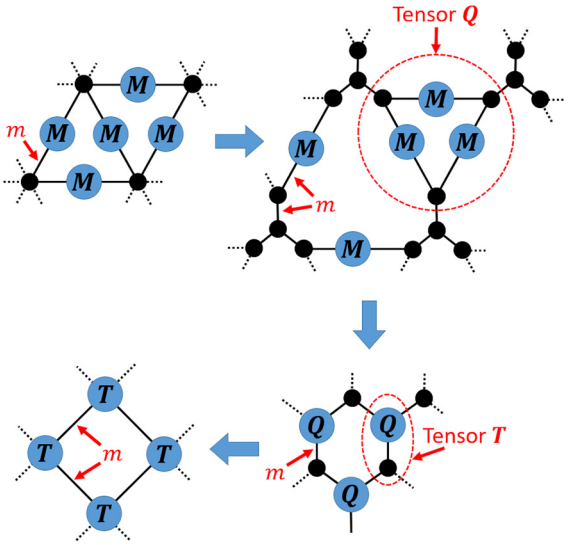

FIG. 3. Graphical representation of the proposed algorithm for constructing a tensor network for triangular lattices.

Obviously, the structure of the T tensor should affect the accuracy of the calculations, so we made a comparison with the previously used approach. First, we traditionally made a comparison using the Ising model as an example. It is known that the critical temperature for a triangular lattice is $T_c = 4/\ln(3)$, and the value of the grand potential at the critical point is $\Omega_I = 3.2025325196\ldots$. Next, we calculated the values of the grand potential at the critical temperature by the TRG method for various χ values. By the formula $\sigma(\chi) = |\Omega_I - \Omega_{\mathrm{TRG}}(\chi)|$, we estimated the error at each value of χ. Figure 4 shows the results.

The proposed transformation leads to an increase in the accuracy of calculations for almost any value of χ. However, the Ising model is very simple, and it is possible that the behavior may be different for more complex models. An exact solution cannot be used in such a situation, so we propose to estimate the error using the following formula:

$$\Delta(\chi) = \sqrt{\frac{\sum_{\mu} |(\Omega_{\chi} - \Omega_{\chi-1})(\Omega_{\chi} - \Omega_{\chi+1})|}{N}}, \qquad (3)$$

where μ is the chemical potential, Ω_χ is the grand potential obtained by the TRG method for a given χ value, and N is the number of chemical potential values taken for calculation. In this work, we took $N = 121$ everywhere. For example, the μ value was varied from -6 to 6, with a step of 0.1.

We proposed a similar method for estimating the error in Ref. [35]. We have shown that the result is less monotonic, but close to the result of comparison with the exact solution. We studied in detail the models with exclusions only up to the third neighbor [35], and for the 4NN and 5NN models, we managed to calculate only adsorption isotherms. Based on these data, we estimated the interval and type of phase transition for them. As shown later in Ref. [25], our estimates turned out to be erroneous. In this regard, we decided to choose the 4NN and 5NN models on a triangular lattice as test models for this work. We demonstrate for them the results achieved by the proposed changes in the algorithm for constructing a tensor network. In addition, we used an

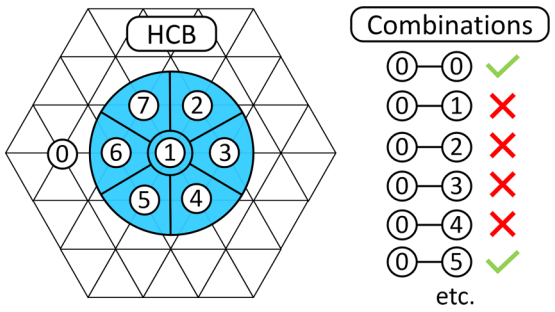

FIG. 5. Representation of a hard-core lattice model.

another approach to determine the possible states of a node for hard-core lattice gas models. It should also improve the accuracy of calculations.

III. TENSOR NETWORK FOR HARD-CORE MODELS

Models with exclusions of several neighbors naturally arise in surface science. Physically, these exclusions are characterized by steric restrictions arising from the adsorption of large molecules. Therefore, it is important to work effectively with models of this type. For example, the presence of exclusions up to the kth neighbor can be interpreted as long-range interactions with the kth neighbor. In this formulation, it is necessary to combine several nodes into one, getting a new node with an increased number of states. Despite the fact that the presence of exclusions makes it possible to ignore some configurations, this leads to a complication of the tensor structure.

However, in this work, we propose to consider the process of node occupation from a chemical point of view. That is, we will not talk about the exclusions, but we will assume that a molecule of a certain size is adsorbed, and it occupies several sites at once. As a result, it is possible to break the adsorbed particle into parts and take them as new states of the node. In a sense, we get a different model, but in fact the model remains the same in terms of probability distribution. Figure 5 visualizes the described process and shows several combinations with an empty node. Now there are forbidden combinations even with an empty node.

The demonstrated version is suitable for describing models with exclusions up to the fifth neighbor. In this case, the new node can take eight states: One of the seven parts of the molecule and an empty node. Note that some of the combinations are compatible with only one neighbor state of the node. For example, to the right of a node in state 5, there can only be a node in state 4. This leads to a simplification of the tensor structure.

Let's call the presented variant of construction a hard-core break (HCB) and compare the results for tensor networks built in different ways using Eq. (3). Note that the TCC approach can be combined with HCB. Thus, we will consider three cases: IRF with joined nodes (the approach used earlier), IRF with HCB, and TCC with HCB. Figure 6 shows graphs of the free-energy error versus χ for the 4NN and 5NN models.

The situation for different models is different, and considered models no longer behave in the same way as the Ising model. The error is noticeably smaller for almost the entire range of considered values of χ for the proposed approaches in the 4NN model. At the same time, the accuracy changes slightly and sometimes not in favor of the proposed approaches for the 5NN model. Despite this, we can conclude that the proposed approaches make it possible to simplify the process of constructing a tensor network and reduce the resulting error even in the case of some complex models.

It is important to note that the proposed approaches can be applied separately from each other. The TCC approach has no limitations and can be applied to any model, including models with finite interactions. The HCB approach requires a hard core, but it remains effective even if there are finite interactions between hard-core particles. As a demonstration of this fact, we will additionally consider a model that can be called intermediate between 4NN and 5NN models. We will call it the 4NN+ model. Suppose that there are exclusions up

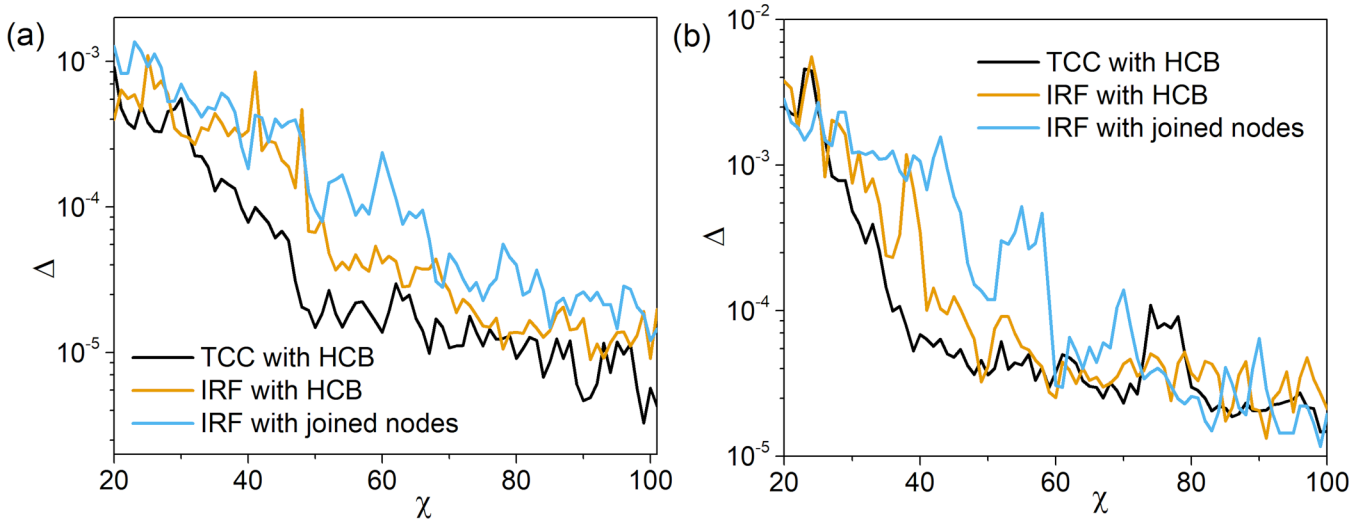

FIG. 6. Comparison of the free-energy error when applying the TRG method to tensor networks constructed in different ways: (a) 4NN model and (b) 5NN model.

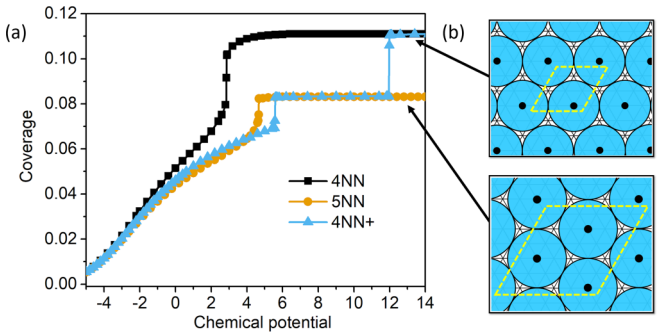

FIG. 7. (a) Adsorption isotherms of the 4NN, 4NN+, and 5NN models and (b) visualization of possible ordered structures. The yellow dashed line indicates the elementary cell of the phase.

to the fourth neighbor, and with the fifth neighbor there is a finite interaction ε. For simplicity, we take the value $\varepsilon = 1$. Physically, this behavior can be characterized as repulsion between neighboring adsorbed molecules of a certain size. For example, for the 3–6 combination of nodes states in the horizontal matrix **M** (in the HCB approach), there will be $\exp(-\beta)$, and not $\exp(0)$ (the combination is allowed), as in the 4NN model or $\exp(-\text{inf})$ (the forbidden combination), as in the 5NN model.

IV. CALCULATION RESULTS

Previously, we were only able to calculate adsorption isotherms for the 4NN and 5NN models [35]. As a result, we made the following assumptions: Only one continuous phase transition occurs in the 4NN model in the region from 2.65 to 2.7, while in the 5NN model there is one first-order phase transition in the region from 4.4 to 4.5. Later, it was shown by the Monte Carlo method using the strip cluster Wang Landau algorithm that a first-order phase transition is observed in both models [25]. In the 4NN model at $\mu_c^{\mathbf{MC}} = 2.8696(2)$, and in the 5NN model at $\mu_c^{\mathbf{MC}} = 4.720(1)$. That is, we incorrectly estimated the type of phase transition in the 4NN model and the regions of phase transitions in both models. Next, we will demonstrate how the application of the proposed approaches changes the situation. In addition, we will demonstrate the results for the 4NN+ model. It has not been studied before, and finite interactions qualitatively distinguish it from the 4NN and 5NN models. Algorithms specialized for investigating only hard-core models often lose their advantage in such a situation. But, the standard TRG algorithm does not have any restrictions on the type of interactions in the system.

Figure 7(a) shows isotherms for all models at once. We will consider the number of adsorbed particles per one lattice site as the coverage. Thus, we will only talk about two ordered structures: Ψ_1 with coverage $\theta = 1/9$ and Ψ_2 with coverage $\theta = 1/12$ [see Fig. 7(b)].

Indeed, a first-order phase transition is observed with the formation of the Ψ_1 phase in the 4NN model. This can be seen from the jump that appears on the adsorption isotherm. Nothing qualitatively changed in the behavior of the 5NN model, and as before, we clearly see the presence of a first-order phase transition. We also managed to obtain high-quality isotherms for the 4NN+ model. First, structure Ψ_2 is formed, and then phase Ψ_1. All transitions are first-order phase transitions. Additionally, we calculated the dependence of entropy and heat capacity on the chemical potential (see Fig. 8).

The entropy behaves in a similar way and reaches close values in the phase transition region in the 4NN and 5NN models, as well as in the first transition in the 4NN+ model. This indicates a similar mechanism for the formation of ordered structures. At the same time, the second phase transition in the 4NN+ model is very different. On the entropy plot, only a slight increase in entropy occurs in the transition region.

In this work, we estimated the critical value of the chemical potential μ_c from the position of the heat capacity peak. Since the main task was only to make a comparison with our earlier estimate, we chose the accuracy to the second decimal place. As can be seen, first-order phase transitions appear on the heat capacity plot as sharp peaks in the transition region. Previously, we did not have enough accuracy to obtain data of sufficient quality, so there was a large spread in the calculated values. Now for the 4NN model at $\chi = 150$, we managed to get the value $\mu_c^{\mathrm{TRG}} = 2.86$. That is, our initial estimate has changed significantly and is now close to the value obtained by the Monte Carlo method in Ref. [25]. For the 5NN model, we had to increase χ to 200 in the phase transition region, as there were noticeable fluctuations in the heat capacity values.

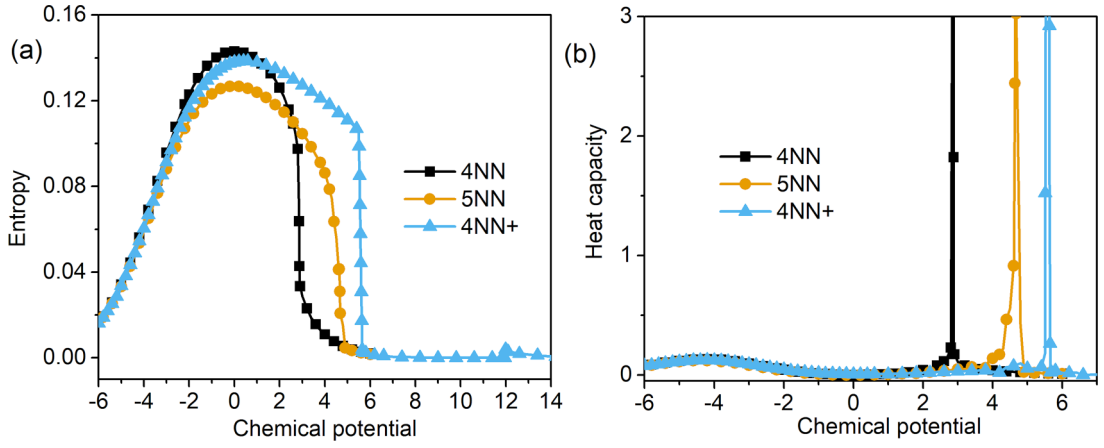

FIG. 8. Dependence of (a) entropy and (b) heat capacity on the chemical potential for all models.

As a result, we got the value $\mu_c^{\mathrm{TRG}} = 4.66$. This is higher than our earlier estimate, but lower than what was obtained by the Monte Carlo method. As shown earlier, the proposed approaches only slightly improve the accuracy for the 5NN model, and this is not enough for a more accurate estimate. In the 4NN+ model, the first peak of heat capacity and susceptibility is observed at the point $\mu_c^{\mathrm{TRG}} = 5.58$. But since the entropy changes weakly in the region of the second phase transition, there are problems with finding the heat capacity peak. Therefore, we determined the position of the second phase transition from the susceptibility peak (we do not present the graph). The peak is observed at the value $\mu_c^{\mathrm{TRG}} = 11.97$.

V. CONCLUSION

We have proposed two self-contained approaches to building tensor networks. The first is tensor contraction with copydots. This approach allows us to simplify the algorithm for constructing a tensor network and, in some cases, leads to a more accurate result when calculating by a tensor renormalization group. The second approach is a hard-core break. It allows us to build a tensor network for hard-core systems without considering long-range interactions. This approach in some models also leads to an increase in the accuracy of calculations.

The possibilities of the proposed approaches were demonstrated on the example of models with exclusions up to the 4NNs and 5NNs. We plotted adsorption isotherms, as well as the dependence of entropy and heat capacity on the chemical potential. The critical values of the chemical potential were determined from the position of the heat capacity peaks, which allowed us to improve our previous estimate of the position of the phase transition point in each model. In addition, we explored a 4NN model with finite repulsions with a fifth neighbor. In a sense, this model is intermediate between 4NN and 5NN models. We found the presence of two first-order phase transitions and made an estimate of the critical values of the chemical potential for each of them.

ACKNOWLEDGMENT

This study was supported by the Russian Science Foundation (Grant No. 22-71-10040).

[1] A. Ibenskas, M. Šimėnas, and E. E. Tornau, Numerical engineering of molecular self-assemblies in a binary system of trimesic and benzenetribenzoic acids, J. Phys. Chem. C **120**, 6669 (2016).

[2] A. Ibenskas, M. Šimėnas, and E. E. Tornau, Multiorientation model for planar ordering of trimesic acid molecules, J. Phys. Chem. C **122**, 7344 (2018).

[3] J. Lisiecki and P. Szabelski, Halogenated anthracenes as building blocks for the on-surface synthesis of covalent polymers: Structure prediction with the lattice Monte Carlo method, J. Phys. Chem. C **125**, 15934 (2021).

[4] D. Nieckarz and P. Szabelski, Theoretical modeling of the surface-guided self-assembly of functional molecules, Chem. Phys. Chem. **21**, 643 (2020).

[5] W. Rżysko, D. Nieckarz, and P. Szabelski, Modeling of the 2D self-assembly of tripod-shaped functional molecules with patchy interaction centers, Adsorption **25**, 75 (2019).

[6] E. Bildanau, J. Pękalski, V. Vikhrenko, and A. Ciach, Adsorption anomalies in a two-dimensional model of cluster-forming systems, Phys. Rev. E **101**, 012801 (2020).

[7] P. Longone, Á. Martín, and J. A. Ramirez-pastor, CO_2-CH_4 exchange process in structure I clathrate hydrates: Calculations of the thermodynamic functions using a flexible 2D lattice-gas model and Monte Carlo simulations, J. Phys. Chem. B **126**, 878 (2022).

[8] P. M. Pasinetti, A. J. Ramirez-Pastor, E. E. Vogel, and G. Saravia, Entropy-driven phases at high coverage adsorption of straight rigid rods on two-dimensional square lattices, Phys. Rev. E **104**, 054136 (2021).

[9] S. Kundu and D. Mandal, Breaking universality in random sequential adsorption on a square lattice with long-range correlated defects, Phys. Rev. E **103**, 042134 (2021).

[10] M. Šimėnas and E. E. Tornau, Pin-wheel hexagons: A model for anthraquinone ordering on Cu(111), J. Chem. Phys. **139**, 154711 (2013).

[11] D. Nieckarz and P. Szabelski, Understanding pattern formation in 2D metal–organic coordination systems on solid surfaces, J. Phys. Chem. C **117**, 11229 (2013).

[12] S. Whitelam, Examples of molecular self-assembly at surfaces, Adv. Mater. **27**, 5720 (2015).

[13] M. Borówko and W. Rżysko, Phase transitions and self-organization of Janus disks in two dimensions studied by Monte Carlo simulations, Phys. Rev. E **90**, 062308 (2014).

[14] K. Kim and T. L. Einstein, Monte Carlo study of the honeycomb structure of anthraquinone molecules on Cu(111), Phys. Rev. B **83**, 245414 (2011).

[15] A. Ibenskas and E. E. Tornau, Statistical model for self-assembly of trimesic acid molecules into homologous series of flower phases, Phys. Rev. E **86**, 051118 (2012).

[16] S. Casalini, C. A. Bortolotti, F. Leonardi, and F. Biscarini, Self-assembled monolayers in organic electronics, Chem. Soc. Rev. **46**, 40 (2017).

[17] G. Vantomme and E. W. Meijer, The construction of supramolecular systems, Science **363**, 1396 (2019).

[18] S. Das, G. Nascimbeni, R. O. de la Morena, F. Ishiwari, Y. Shoji, T. Fukushima, M. Buck, E. Zojer, and M. Zharnikov, Porous honeycomb self-assembled monolayers: Tripodal adsorption and hidden chirality of carboxylate anchored triptycenes on Ag, ACS Nano **15**, 11168 (2021).

[19] D. P. Goronzy *et al.*, Supramolecular assemblies on surfaces: Nanopatterning, functionality, and reactivity, ACS Nano **12**, 7445 (2018).

[20] R. Yi, Y. Mao, Y. Shen, and L. Chen, Self-assembled monolayers for batteries, J. Am. Chem. Soc. **143**, 12897 (2021).

[21] P. Szabelski, D. Nieckarz, and W. Rżysko, Structure formation in 2D assemblies comprising functional tripod molecules with reduced symmetry, J. Phys. Chem. C **121**, 25104 (2017).

[22] Z. Wojtkowiak and G. Musiał, Cluster Monte Carlo method for the 3D Ashkin–Teller model, J. Magn. Magn. Mater. **500**, 166365 (2020).

[23] A. A. A. Jaleel, J. E. Thomas, D. Mandal, Sumedha, and R. Rajesh, Rejection-free cluster Wang-Landau algorithm for hard-core lattice gases, Phys. Rev. E **104**, 045310 (2021).
[24] A. A. A. Jaleel, D. Mandal, and R. Rajesh, Hard core lattice gas with third next-nearest neighbor exclusion on triangular lattice: One or two phase transitions? J. Chem. Phys. **155**, 224101 (2021).
[25] A. A. A. Jaleel, D. Mandal, J. E. Thomas, and R. Rajesh, Freezing phase transition in hard-core lattice gases on the triangular lattice with exclusion up to seventh next-nearest neighbor, Phys. Rev. E **106**, 044136 (2022).
[26] A. J. Phares and F. J. Wunderlich, Coadsorption of monomers and dimers with first neighbour interactions on square lattices, Phys. Lett. A **226**, 336 (1997).
[27] S. S. Akimenko, V. F. Fefelov, A. V. Myshlyavtsev, and P. V. Stishenko, Remnants of the devil's staircase of phase transitions in the model of dimer adsorption at nonzero temperature, Phys. Rev. B **97**, 085408 (2018).
[28] G. Li, K. H. Pai, and Z.- C. Gu, Tensor-network renormalization approach to the q-state clock model, Phys. Rev. Res. **4**, 023159 (2022).
[29] R. Kaneko and I. Danshita, Tensor-network study of correlation-spreading dynamics in the two-dimensional Bose-Hubbard model, Commun. Phys. **5**, 65 (2022).
[30] Y. Ito, D. Kadoh, and Y. Sato, Tensor network approach to 2D Lorentzian quantum Regge calculus, Phys. Rev. D **106**, 106004 (2022).
[31] C. McKeever and M. H. Szymańska, Stable iPEPO Tensor-Network Algorithm for Dynamics of Two-Dimensional Open Quantum Lattice Models, Phys. Rev. X **11**, 021035 (2021).
[32] G. Magnifico, T. Felser, P. Silvi, and S. Montangero, Lattice quantum electrodynamics in (3+1)-dimensions at finite density with tensor networks, Nat. Commun. **12**, 3600 (2021).
[33] C.- M. Jian, B. Bauer, A. Keselman, and A. W. W. Ludwig, Criticality and entanglement in nonunitary quantum circuits and tensor networks of noninteracting fermions, Phys. Rev. B **106**, 134206 (2022).
[34] P. Helms and G. K.- L. Chan, Dynamical Phase Transitions in a 2D Classical Nonequilibrium Model via 2D Tensor Networks, Phys. Rev. Lett. **125**, 140601 (2020).
[35] S. S. Akimenko, V. A. Gorbunov, A. V. Myshlyavtsev, and P. V. Stishenko, Tensor renormalization group study of hard-disk models on a triangular lattice, Phys. Rev. E **100**, 022108 (2019).
[36] M. Levin and C. P. Nave, Tensor Renormalization Group Approach to Two-Dimensional Classical Lattice Models, Phys. Rev. Lett. **99**, 120601 (2007).
[37] Z. Y. Xie, H. C. Jiang, Q. N. Chen, Z. Y. Weng, and T. Xiang, Second Renormalization of Tensor-Network States, Phys. Rev. Lett. **103**, 160601 (2009).
[38] G. Evenbly and G. Vidal, Tensor Network Renormalization, Phys. Rev. Lett. **115**, 180405 (2015).
[39] Z. Y. Xie, J. Chen, M. P. Qin, J. W. Zhu, L. P. Yang, and T. Xiang, Coarse-graining renormalization by higher-order singular value decomposition, Phys. Rev. B **86**, 045139 (2012).
[40] T. Nishino and K. Okunishi, Corner transfer matrix renormalization group method, J. Phys. Soc. Jpn. **65**, 891 (1996).
[41] T. Nishino and K. Okunishi, Corner transfer matrix algorithm for classical renormalization group, J. Phys. Soc. Jpn. **66**, 3040 (1997).
[42] S. Yang, Z.- C. Gu, and X. -G. Wen, Loop Optimization for Tensor Network Renormalization, Phys. Rev. Lett. **118**, 110504 (2017).
[43] M. Hauru, C. Delcamp, and S. Mizera, Renormalization of tensor networks using graph-independent local truncations, Phys. Rev. B **97**, 045111 (2018).
[44] S. Cheng, L. Wang, T. Xiang, and P. Zhang, Tree tensor networks for generative modeling, Phys. Rev. B **99**, 155131 (2019).
[45] R. Orús, A practical introduction to tensor networks: Matrix product states and projected entangled pair states, Ann. Phys. **349**, 117 (2014).
[46] J. D. Biamonte, S. R. Clark, and D. Jaksch, Categorical tensor network states, AIP Advances **1**, 042172 (2011).
[47] H. H. Zhao, Z. Y. Xie, Q. N. Chen, Z. C. Wei, J. W. Cai, and T. Xiang, Renormalization of tensor-network states, Phys. Rev. B **81**, 174411 (2010).